Information Fusion 38 (2017) 55–64

Contents lists available at ScienceDirect

Information Fusion

journal homepage: www.elsevier.com/locate/inffus

Information fusion for efficient target detection in large-scale surveillance Wireless Sensor Networks

Andrea Abrardo[a], Marco Martalò[b,c], Gianluigi Ferrari[b,*]

[a] Department of Information Engineering, University of Siena, Italy
[b] Wireless Ad-hoc and Sensor Networks (WASN) Laboratory, Department of Information Engineering, University of Parma, Italy
[c] SMART Engineering Solutions & Technologies (SMARTEST) Research Center, E-Campus University, Novedrate (CO), Italy

ARTICLE INFO

Article history:
Received 3 August 2016
Revised 15 December 2016
Accepted 1 February 2017
Available online 3 February 2017

Keywords:
Wireless Sensor Network (WSN)
ELectronic-signals INTelligence (ELINT)
False Alarm (FA)
Correct Detection (CD)
Clustering
Energy consumption

ABSTRACT

In this paper, we consider a surveillance scenario, where nodes of a Wireless Sensor Network (WSN) cooperate to detect an event of interest, e.g., the presence of a mobile target in a monitored region. The considered scenario refers, for example, to ELectronic-signals INTelligence (ELINT), since detection is based on sensing the presence of anomalous electromagnetic signals in the monitored area. Leveraging previous results in the field of cognitive wireless networking, we derive proper decision and fusion strategies. We investigate both clustered (where no direct communication between sensors and the Communication and Control center, C2, is allowed and intermediate data fusion is performed at Cluster Heads, CHs) and unclustered (with direct communications between sensor nodes and the C2). System performance is analyzed in terms of False Alarm (FA)/Correct Detection (CD) probabilities and energy consumption, quantifying inherent tradeoffs between these performance indicators.

1. Introduction

Wireless Sensor Networking (WSN) is one of the most promising technologies that have applications ranging from health care to military scenarios [1], because of the following appealing features: low installation cost, unattended network operations, etc. Target detection is a critical task for WSN-based surveillance applications. Detection of unauthorized targets in a monitored area can be carried out by monitoring the presence of a signal of interest, which may be of different nature, e.g., seismic, electromagnetic, etc [2].

Different target detection schemes for surveillance scenarios have been proposed in the literature. In many cases, the main performance indicators used for system design are related to the network detection capabilities, e.g., the probability that the target presence is correctly detected (see, e.g., [3,4] and references therein). However, WSNs for target surveillance applications have to cope with limitations in terms of energy consumption and latency. Therefore, various approaches have been proposed in the literature to design WSN-based solutions for target detection that also minimize the overall latency [5] or the energy consumption [6]. Event-triggered communication/networking protocols have also been exploited in other applications, e.g., in distributed consensus, where rapid convergence without communication burden is desired [7–9].

Target detection and event-based detection are problems strictly related to the field of cognitive networking, where some unlicensed secondary nodes need to detect the presence of licensed primary nodes' activities [10]. In cooperative spectrum sensing, secondary nodes send their data (raw sensed data or preliminary decisions) to a common collector, which uses such data to take a decision on the occupation of the considered bandwidth portion. In [11], the authors consider a single-hop collaborative cognitive network and derive optimal fusion strategies with and without the knowledge of the nodes' positions in the network.

In this paper, we devise energy-efficient information fusion strategies triggered by the detection of a mobile target, e.g., an Unmanned Aerial Vehicle (UAV). We consider an ELectronic-signals INTelligence (ELINT) scenario, where the event detection is based on the radio signal emitted by the mobile target [12]. Motivated by the recent advances in SubGHz communication technologies, which allow relatively inexpensive wireless devices to communicate at distances of the order of kilometers [13], we first consider a scenario with direct communications between the WSN nodes and the Communication and Control center (C2). In order to reduce the energy consumption and prolonging the network lifetime, we consider the presence of clustering, so that the communication range can be reduced. In this case, local decisions are collected by a Cluster Head (CH) using short-range communications. Proper

* Corresponding author.
E-mail addresses: abrardo@dii.unisi.it (A. Abrardo), marco.martalo@unipr.it (M. Martalò), gianluigi.ferrari@unipr.it (G. Ferrari).

http://dx.doi.org/10.1016/j.inffus.2017.02.002
1566-2535/

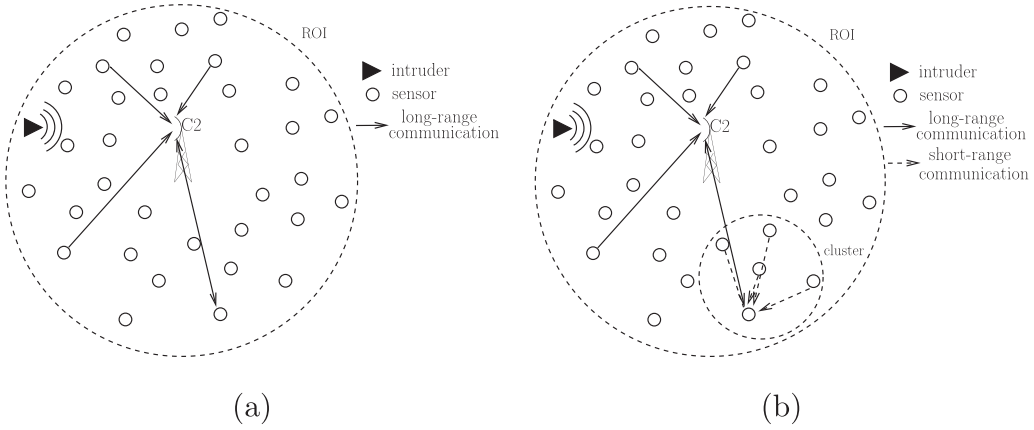

Fig. 1. Illustrative scenarios of interest for mobile target detection: (a) direct sensor-C2 communications and (b) clustered (2-hop) topology.

intermediate (at the CHs) and final (at the C2) fusion rules are designed. Although event-based communication/networking protocols and target detection are well-known problems, the novelty of our work can be summarized as follows. First, we exploit a duality between cognitive wireless networking and WSN-based target detection systems to efficiently tackle the target detection problem. Moreover, in this context we propose an analytical framework which allows to evaluate two different performance indicators: (i) detection capability, in terms of False Alarm (FA) and Correct Detection (CD) probabilities; and (ii) the overall network energy consumption. The obtained results show the inherent tradeoff between these two performance indicators.

The rest of the paper is structured as follows. In Section 2, we present the system model. In Section 3, we derive an analytical performance framework, in terms of FA/CD probabilities and energy consumption. In Section 4, a comparative (clustered-vs-unclustered and simulation-based-vs-analytical) performance evaluation is carried out. Finally, concluding remarks are given in Section 5.

2. System model

2.1. Reference scenarios

In Fig. 1, the two illustrative scenarios of interest for mobile target (denoted as "intruder") detection are shown. In both cases, the C2 is placed at the center of the Region Of Interest (ROI), which is assumed to be a circular region with a given radius R, while N sensors are independent and identically distributed (i.i.d.), according to a spatial uniform distribution, in the ROI. The proposed approach can, however, be generalized to other types of ROIs (at the cost of a reduced analytical tractability) and the C2 could be placed outside the ROI. For the sake of simplicity, in the remainder of this paper we will assume that $R = 1$ (normalized radius, e.g., 1 km), i.e., the ROI is a circle with unitary radius. The two scenarios of interest in Fig. 1 refer to two different topologies. In case (a), one-hop long-range communications between all N sensors and the C2 are allowed. Long-range communications are motivated by the recent advances in SubGHz communication technologies, which allow relatively inexpensive wireless devices to communicate at distances of the order of kilometers [13]. In order to save energy, in case (b) nodes are grouped into a fixed number (denoted as N_c) of clusters and, in each cluster, one of the inner nodes acts as CH. Short-range communications (e.g., IEEE 802.15.4 or IEEE 802.11) between sensors and CHs are used inside the clusters, whereas long-range communications between CHs and the C2 are allowed. It is worth observing that in case (b) each CH is likely to be always active (in order to be able to receive reports from the controlled nodes): hence, it consumes more energy than other nodes in its cluster. Therefore, if the CH is kept fixed, its energy will deplete sooner than those of the other non-CH nodes. In order to equalize the energy consumption within a cluster, we will adopt a CH rotation strategy, giving all nodes the same probability of becoming CH.

Denoting the set of nodes belonging to the ith cluster ($i = 1, \ldots, N_c$) as $\mathcal{C}_i$, it follows that

$$\sum_{i=1}^{N_c} |\mathcal{C}_i| = N$$

whereas $|\mathcal{C}_i|$ is the size of the ith cluster. In Section 4, clusters will be formed (with a simulation-based approach) through the well-known k-means algorithm [14,15]. Although several clustering algorithms can be considered, k-means was selected as it leads, on average, to uniform clusters, i.e., $\overline{|\mathcal{C}_i|} = \lfloor N/N_c \rceil$, $\forall i \in \{1, \ldots, N_c\}$, where $\lfloor \cdot \rceil$ denotes the integer nearest to the argument. We remark that cluster formation goes beyond the scope of this paper.

As anticipated in Section 1, the goal of the deployed WSN (either clustered or unclustered) is to detect the presence of a target from its electromagnetic emissions (namely, radio communications). This is meaningful in several scenarios, e.g., in ELINT or cognitive radio applications. In particular, target detection is performed by scanning a proper radio bandwidth, over which the target is assumed to transmit its own radio signal with fixed power[1] P_T—relaxing this assumption leads to a further generalization of our approach and is the subject of our current research activity. Without loss of generality, we assume that all sensors in the ROI may sense, if present, an electromagnetic signal emitted by the target. In particular, we assume that each node carries out a spectrum swipe over a sufficiently large number of subbands. In each subband, target presence (i.e., its electromagnetic emission) can be modeled by a Bernoulli random variable S, which can assume the value $S_0 = 0$ (no target) or $S_1 = 1$ (target is present) with probabilities p_0 and $p_1 = 1 - p_0$, respectively. In particular, in the applications of interest it holds that $p_1 \ll 0.5$. We assume that the electromagnetic signal emitted by the target is received by the nodes in the WSN according to a classical cellular-like model, accounting for path-loss and shadowing—this is realistic, given the considered scenarios in Fig. 1.

[1] In the remainder of this paper, the dimensional unit of power is not explicitly indicated, as the performance will be investigated in terms of normalized values (as discussed in more detail later). However, realistic values are expected to be on the order of mWs and tens of mWs for short-range and long-range communications, respectively.

From a statistical point of view, for each subband of the considered scanned spectrum, event detection at each node is based on binary hypothesis testing. On the basis of the assumptions above, the kth sensor node ($k = 1, \ldots, N$) has to distinguish between two independent Gaussian sequences:

$$\mu_k(\ell) = \begin{cases} s_k(\ell) + n_k(\ell) & \text{if } S = S_1 \\ n_k(\ell) & \text{if } S = S_0 \end{cases} \qquad \ell = 1, \ldots, m \tag{1}$$

where: m is the number of observed consecutive samples in a single sensing "block" used to take a binary decision on the presence/absence of a signal; $\{s_k(\ell)\}$ are the samples of the signal received by the kth sensor (and emitted by the target); and the noise terms $\{n_k(\ell)\}$ are modeled as i.i.d. zero-mean complex Gaussian random variables with fixed variance P_N (corresponding to the noise power), constant for all sensors. Note that an implicit assumption in (1) is that the phenomenon status does not change over m consecutive observations—this is reasonable in ELINT scenarios with sufficiently slowly moving (with respect to the nodes' sampling rate) target. Since it is reasonable to assume that the sensors have no a-priori knowledge about the modulation and pulse shaping formats adopted by the target, in (1) $\{s_k(\ell)\}$ is modeled a sequence of i.i.d. zero-mean complex Gaussian random variables with variance $P_R^{(k)}$ (corresponding to the received power) [16, Section 4.2.1]. The power $P_R^{(k)}$ depends on the transmit power P_T and on the path-loss and shadowing terms characterizing the link between the target and the kth node. In the following, we assume that path-loss and shadowing terms are constant over all m consecutive observations: this is compliant with the previous assumption of sufficiently slowly varying wireless scenarios.

Describing the bidimensional space of reference (i.e., the ROI) as the complex plane, we denote as v_k and v_t the positions of the kth sensor and of the target, respectively. We assume that there is no knowledge of nodes' positions in the network—this is an extension left for future work. The Euclidean distance d_k between the target and the kth sensor is $d_k = |v_t - v_k|$. Therefore, the sensing Signal-to-Noise Ratio (SNR) experienced by the kth sensor node, with respect to the target, can be expressed as follows:

$$\gamma_k(d_k, h) = \frac{P_R^{(k)}}{P_N} = \frac{K h_k P_T}{P_N d_k^{\alpha}} \tag{2}$$

where the Friis formula for the received power has been used [17], in which α is the path-loss attenuation exponent (adimensional, in the range 2÷4), K is the gain at 1 m from the transmitter (i.e., the target), and h_k is the log-normal shadowing coefficient of the link between the target and the kth sensor with standard deviation σ (adimensional, dB).

The kth sensor uses the observables $\{\mu_k(\ell)\}$ to make a local binary decision X_k. Under the observation model (1), an Energy Detection (ED) scheme is the optimal detector in the Neyman–Pearson sense [18]. In particular, the following decision variable has to be evaluated:

$$W_k = \sum_{\ell=1}^{m} |\mu_k(\ell)|^2 \tag{3}$$

and the binary decision rule at the sensor is given by

$$X_k = U(W_k - \tau) = \begin{cases} 1 & \text{if } W_k \geq \tau \\ 0 & \text{if } W_k < \tau \end{cases} \tag{4}$$

where τ is a properly selected decision threshold and $U(\cdot)$ is the unit-step function.

2.2. Simplified clustering model

In order to derive an analytical approach for system performance evaluation, it is necessary to introduce a simplified clustering model (with respect to a more realistic, but simulation-based, k-means-based approach), especially to characterize the generic position of the target inside the ROI. To this aim, we adopt a simple "homogeneous" model according to which: (i) each cluster covers a circular area with radius $r = R/\sqrt{N_c}$ and (ii) the clusters' centers are regularly arranged inside the ROI following an hexagonal packing with radius r. We denote by $V_{C,i}$ ($i = 1, \ldots, N_c$) the complex representation of the coordinates of the center of the ith circular cluster. Note that, in the considered model, there is a slight overlapping among adjacent clusters, which is due to the assumption of circular clusters. Hence, this model tends to slightly overestimate the average cluster size. Considering the number of nodes $|\mathcal{C}_i|$ belonging to cluster $\mathcal{C}_i$, we make the assumption of uniform distribution of the nodes inside the clusters, i.e., a node belongs to a given cluster with probability $1/N_c$. Accordingly, the Probability Mass Function (PMF) of the number of nodes in a cluster can be written as

$$p_n = P(|\mathcal{C}_i| = n) = \binom{N}{n} \left(\frac{1}{N_c}\right)^n \left(1 - \frac{1}{N_c}\right)^{N-n}. \tag{5}$$

Note that in the proposed clustering model the correlation among different clusters are not taken into account. In fact, we assume, for simplicity, that the numbers of sensors in different clusters are independent. However, since the number of sensors N in the ROI is fixed, the numbers of sensors in different clusters are strictly correlated. For instance, if $N_c = 2$ and one of cluster has a small number of sensors, then the other cluster is forced to have a large number of sensors. Although this effect is not captured in our analytical model, simulation results show good trend-wise agreement.

The simplified clustering model introduced above allows to investigate the system performance analytically. Nevertheless, this model captures the essence of the detection problem at hand: in fact, in Section 4 simulation-based and analytical performance results will be in very good agreement.

2.3. Energy consumption model

Energy consumption is an important issue for WSNs formed by battery-equipped sensor nodes. In order to determine the average energy consumption at each node, it is necessary to identify the various states of a node and the corresponding energy costs. To this aim, we consider a Carrier Sense Multiple Access with Collision Avoidance (CSMA/CA) random access in the entire network (in the absence of clustering) or in each cluster (in the presence of clustering). Being the WSN deployed for surveillance purposes, we assume the use of beacons to improve the performance of the random access protocol. In order to simplify the energy consumption model (since this is not the focus of our paper), we assume that energy consumption complies with the well-established model for the IEEE 802.15.4 standard with beacon-enabled channel access and Guaranteed Time Slot (GTS) to each node [19]—we remark that this model is applicable, with minor modifications, also to other beacon-enabled CSMA/CA-based networks. This access protocol allows to guarantee low latency transmissions, which is a very important requirement for the scenario at hand.

As typical in surveillance scenarios, we assume that the C2 withdraws energy from the power grid and, as such, energy consumption is not a concern. Therefore, in the remainder we focus on the energy consumption at sensor nodes (in both clustered and unclustered scenarios) and at the CHs (in clustered scenarios).

2.3.1. Clustered scenario

In each cluster, the CH plays the role of coordinator and, as such, is responsible for both managing the superframe structure and sending the periodic beacon at the beginning of each superframe. The superframe is divided into an active period (with du-

ration T_A) and an inactive period. During the inactive period, all nodes enter into a sleep node, thus saving energy.

In the considered sensing scenario, we assume that part of the active period is exploited by the nodes to sense the channel with the aim of detecting the possible presence of the target. Hence, we assume that the remaining part of the active period is divided into a proper number (denoted as M) of time slots, each with duration T_M: one of them is used to send the beacon (from the CH to the nodes of its cluster), while the remaining $M-1$ slots (the number of nodes in the cluster must not be larger than $M-1$) are assigned by the CH to the controlled nodes. A dedicated slot is either used by the node to inform the CH that a target has been detected or is left unused (if no target has been detected). As for the transmissions from the CHs towards the C2, we assume that they occur following the same beacon-enabled strategy with GTSs of the clusters, with the C2 playing the role of coordinator.

As shown in [20], a node can be in one of the following five states: transmit (Tx), receive (Rx), channel sense (CS), idle, and sleep. The various states are characterized by different average power (and, thus, energy) consumptions. In particular, for short range communications, i.e., intra-cluster communications between sensor nodes and CH, we can assume that Tx, Rx, and CS are characterized by the same power level, referred to as P_M in the following. This is reasonable in IEEE 802.15.4-based networks, where the corresponding energy consumptions are all on the order of a few milliwatts [21,22]. Considering long-range communications, we assume that the CHs use a transmit power γ times higher than in the case of inter-cluster communications, i.e., γP_M. The power consumptions in the idle and sleep states are assumed to be negligible with respect to those in the other states.

Owing to the above assumptions, one can derive the average energy consumed by a sensor node in a superframe: we denote this energy as E_S, where S refers to the sensing status (presence/absence of detection). In each superframe, regardless of the sensing status, a sensor node consumes energy to read the beacon and to perform channel sensing. In the presence of target detection ($S=S_1$), further energy is consumed to transmit the positive decision (i.e., estimated target presence) from the node to the CH. Hence, denoting by β the time dedicated to target sensing expressed in terms of equivalent time slots, the overall energy consumption at a sensor node is:

$$E_S = \begin{cases} E_{S_1} = (2+\beta)P_{\mathrm{M}}T_{\mathrm{M}} & \text{if } S=S_1 \\ E_{S_0} = (1+\beta)P_{\mathrm{M}}T_{\mathrm{M}} & \text{if } S=S_0 \end{cases} \tag{6}$$

where: $P_{\mathrm{M}}T_{\mathrm{M}}$ is the energy consumed in Rx state (receiving the beacon); $P_{\mathrm{M}}\beta T_{\mathrm{M}}$ is the energy consumed in the CS state; and $P_{\mathrm{M}}T_{\mathrm{M}}$ is the energy consumed in Tx state (if transmitting a decision to the CH).

We now evaluate the energy, denoted as E_{CH}, consumed by a CH during a superframe. We preliminary observe that in the active period of a superframe a CH is always active, being either in the Rx state (while receiving packets from sensor nodes) or in the Tx state (while transmitting the beacon). Moreover, assuming that a CH has sensing capabilities, energy is consumed also to perform channel sensing. Finally, a CH consumes energy for packet transmission toward the C2 if a target is detected inside the cluster. The energy consumed by a CH during a superframe can thus be expressed as follows:

$$E_{\mathrm{CH}} = \begin{cases} E_{\mathrm{CH},1} = (\gamma+M+\beta)P_{\mathrm{M}}T_{\mathrm{M}} & \text{with target detection} \\ E_{\mathrm{CH},0} = (M+\beta)P_{\mathrm{M}}T_{\mathrm{M}} & \text{without target detection.} \end{cases} \tag{7}$$

In particular, in (7) it has been assumed that while the Tx power (to send a decision to the C2) increases to γP_{M}, the Rx power (to receive the beacon from the C2) remains fixed to P_{M}. The estimated presence or absence of the target inside a cluster depends on the local (inside a cluster) fusion rule adopted at the CH and will be discussed later.

2.3.2. Unclustered scenario

In the absence of clustering, i.e., in a scenario where the C2 plays the role of coordinator for all nodes in the ROI, the energy consumed by a sensor node in a superframe, denoted as $E_S^{(f)}$, can be directly obtained from (6) by taking into account that the transmit power to reach the C2 is γP_{M}, thus obtaining:

$$E_S^{(f)} = \begin{cases} E_{S_1}^{(f)} = (\gamma+1+\beta)P_{\mathrm{M}}T_{\mathrm{M}} & \text{if } S=S_1 \\ E_{S_0}^{(f)} = (1+\beta)P_{\mathrm{M}}T_{\mathrm{M}} & \text{if } S=S_0. \end{cases} \tag{8}$$

2.4. Fusion rule

2.4.1. Clustered scenario

The optimum fusion strategy at the CH derives from the application of the Neyman–Pearson criterion and requires the evaluation of the likelihood ratio between the probabilities of observing the reports received from the nodes under the two hypothesis S_1 and S_0. Denoting $Q_i = |\mathcal{C}_i|$ as the number of nodes in ith cluster, the likelihood ratio can be expressed as follows:

$$\mathcal{L}(X_1,\ldots,X_{Q_i}) = \frac{P(X_1,\ldots,X_{Q_i}|S_1)}{P(X_1,\ldots,X_{Q_i}|S_0)} \underset{S_0}{\overset{S_1}{\gtrless}} \lambda_i \tag{9}$$

where λ_i is a decision threshold which, in general terms, should be optimized for the ith cluster (e.g., depending on the value of Q_i). According to the considered communication setup, only the nodes which detect the target transmit to the CH: this is equivalent to considering that all the other nodes send a null report. Note that under hypothesis S_1, $\{X_k\}$ are not independent, since they jointly depend on the position V_{T} of the target. However, owing to the symmetry of the considered scenario and to the lack of a-priori information about the positions of the nodes, the probability associated with the reports received by the CH is permutation-invariant, i.e., $P(X_1,\ldots,X_{Q_i}|S_1) = P(\Sigma(X_1,\ldots,X_{Q_i})|S_1)$ for any permutation Σ. Then, it follows that $\mathcal{L}(X_1,\ldots,X_{Q_i})$ depends only on the number of ones contained in $(X_1,\ldots,X_{Q_i})$, i.e., on the value of the following random variable:

$$X_{\mathrm{tot}}^{(i)} = \sum_{k=1}^{Q_i} X_k. \tag{10}$$

Therefore, $X_{\mathrm{tot}}^{(i)}$ is a sufficient statistic for detection in the ith cluster. Due to the nature of the problem at hand, we also argue that $\mathcal{L}(X_1,\ldots,X_{Q_i})$ is a monotonically increasing function of $X_{\mathrm{tot}}^{(i)}$, thus leading to the following reformulation of the optimal decision rule at the CH:

$$X_{\mathrm{tot}}^{(i)} \underset{S_0}{\overset{S_1}{\gtrless}} T_{\mathrm{CH}} \tag{11}$$

where T_{CH} is a threshold whose value must be selected to obtain the desired FA and CD probabilities at the CH. Note that, unlike the general formulation in (9), in (11) the decision threshold is independent of the cluster index i: this is consistent with the simplified clustering model introduced in Section 2.2.

As for the final decision rule at the C2, following the same considerations outlined above, it is straightforward to express the optimal decision rule as follows:

$$Y_{\mathrm{tot}} = \sum_{i=1}^{N_c} f_{c_2}(X_{\mathrm{tot}}^{(i)}) \underset{S_0}{\overset{S_1}{\gtrless}} T_{\mathrm{C2}} \tag{12}$$

where T_{C2} is a threshold to be properly selected in order to obtain the final FA and CD probabilities and

$$f_{c_2}(X_{\text{tot}}^{(i)}) = \begin{cases} 1 & \text{if } X_{\text{tot}}^{(i)} \geq T_{CH} \\ 0 & \text{if } X_{\text{tot}}^{(i)} < T_{CH}. \end{cases}$$

2.4.2. Unclustered scenario

In the absence of clustering, i.e., in the presence of direct communications between the sensor nodes and the C2, the decision rule at the C2 can be easily obtained from the derivation in the clustered scenario. In particular, from (10) one can write:

$$Y_{\text{tot-unc}} = \sum_{k=1}^{N} X_k \underset{S_0}{\overset{S_1}{\gtrless}} T_{\text{C2-u}} \tag{13}$$

where the value of the decision threshold $T_{\text{C2-u}}$ has to be properly selected.

3. Analytical performance evaluation

3.1. Local performance: CD and FA probabilities at a sensor node

The local FA and CD probabilities, under the proposed ED scheme, can be defined as follows (see, e.g., [23] and references therein):

$$P_{\text{FA}}^{(k)} \triangleq P(X_k = 1|S_0) = P(W_k \geq \tau|S_0)$$
$$P_{\text{CD}}^{(k)} \triangleq P(X_k = 1|S_1) = P(W_k \geq \tau|S_1).$$

Using straightforward manipulations, the local FA and CD probabilities at a sensor with ED can then be expressed as [18]

$$P_{\text{FA}}^{(k)} = \Gamma_{\text{u}}(m\tau_{\text{N}}, m)$$
$$P_{\text{CD}}^{(k)} = \Gamma_{\text{u}}\left(\frac{m\tau_{\text{N}}}{1+\gamma_k(d_k,h)}, m\right) \tag{14}$$

where $\tau_{\text{N}} = P_{\text{N}}\tau$ is the normalized threshold with respect to the noise power and $\Gamma_{\text{u}}(a,n) \triangleq \int_a^{\infty} x^{n-1}e^{-x}\,\text{d}x/(n-1)!$ is the upper incomplete gamma function [24].

Note that the FA probability is the same for all sensors and does not depend on their distances from the target: we thus denote $P_{\text{FA}}^{(k)} = P_{\text{FA}},\ \forall k \in \{1,2,\ldots,N\}$. The CD probability, instead, depends on the distance d_k and on the shadowing term h_k. Averaging with respect to the statistical distribution of the shadowing term, the following expression for the average CD probability at distance d_k can be obtained:

$$\begin{aligned}\overline{P}_{\text{CD}}(d_k) &= \mathbb{E}_{h_k}\left[P_{\text{CD}}^{(k)}(d_k,h_k)\right] \\ &= \frac{1}{\sqrt{2\pi\sigma^2}}\int_{-\infty}^{\infty}\Gamma_{\text{u}}\left(\frac{m\tau_{\text{N}}}{1+\gamma_k(d_k,10^{S/10})}, m\right)e^{-\frac{S^2}{2\sigma^2}}\,\text{d}S\end{aligned} \tag{15}$$

which has no closed-form solution, but can be numerically evaluated. Note that, since the average CD probability in (15) is a function of d_k only, for notational simplicity we have removed the superscript k.

3.2. Global performance

3.2.1. Preliminary geometric considerations

Denote the position of the target (in the complex plane centered at the C2) as $V_{\text{T}} = Xe^{j2\pi\Phi}$. Owing to the circular ROI with unitary radius $R = 1$, it follows that $\Phi \sim \text{Unif}(0,1)$ and the Probability Density Function (PDF) of X can be written as:

$$f_X(\delta) = \begin{cases} 2\delta & \delta \in (0,1) \\ 0 & \text{otherwise.} \end{cases} \tag{16}$$

Owing to the circular symmetry of the scenario, we can consider $\Phi = 0$: therefore, $V_{\text{T}} = X$. Denote now: R_i as the distance between the center of ith cluster and the target, i.e., $R_i = R_i(X) = \sqrt{|V_{\text{C},i} - X|^2}$; D as the distance between a generic node belonging to cluster i and the target at position V_{T}. The PDF of D, denoted as $f_D(\rho|R_i(X) = r_i(x))$, can be derived by considering two different cases, depending on the relative position (outside or inside) of the target with respect to the ith cluster.

In the *first case*, the target is outside the ith cluster, i.e., $r_i(x) > r$, where $r = R/\sqrt{N_c} = 1/\sqrt{N_c}$. This situation is illustrated in Fig. 2(a). For $\rho < r_i(x) - r$, the annulus centered at V_{T} with inner radius ρ and outer radius $\rho + d\rho$ is outside the cluster with radius 1 and, therefore, we have $f_D(\rho|r_i(x)) = 0$. On the other hand, when $r_i(x) - r \leq \rho < r_i(x) + r$ only a portion of the annulus lies within the cluster and, therefore, $f_D(\rho|r_i(x))$ is obtained by dividing the area of this portion and the area of surface of the cluster. Through simple geometric considerations, one obtains:

$$f_D(\rho|r_i(x)) = \frac{2\rho}{\pi}\cos^{-1}\left(\frac{\rho^2 + r_i^2(x) - r^2}{2\rho r_i(x)}\right). \tag{17}$$

Finally, for $\rho \geq r_i(x) + r$ the annulus is fully outside the cluster and, hence, $f_D(\rho|r_i(x)) = 0$.

In the *second case*, the target is inside the ith cluster, i.e., $r_i(x) \leq r$. This situation is illustrated in Fig. 2(b). Following similar considerations as above, we note that for $\rho < r - r_i(x)$ the annulus centered at V_{T} with inner radius ρ and outer radius $\rho + d\rho$ is fully included into the cluster and, therefore, it follows that $f_D(\rho|r_i(x)) = 2\rho$. On the other hand, when $r - r_i(x) \leq \rho < r_i(x) + r$ only a portion of the annulus lies within the cluster and, in this case, $f_D(\rho)$ can be expressed as follows:

$$f_D(\rho|r_i(x)) = \frac{2\rho}{\pi}\left[\pi - \cos^{-1}\left(\frac{r^2 - \rho^2 - r_i^2(x)}{2\rho r_i(x)}\right)\right]. \tag{18}$$

Finally, for $\rho \geq r_i(x) + r$ the annulus is fully outside the cluster and, hence, $f_d(\rho|r_i(x)) = 0$.

3.2.2. CD And FA probabilities

Denote as $\overline{P}_{\text{CD}}(r_i(\delta))$ the average probability of CD of a generic node belonging to the ith cluster, averaged over all possible distances d with respect to the target, for a given target position $X = \delta$. One can thus write:

$$\overline{P}_{\text{CD}}(r_i(\delta)) = \int_{\rho}\overline{P}_{\text{CD}}(\rho)f_d(\rho|r_i(\delta))\text{d}\rho \tag{19}$$

where $\overline{P}_{\text{CD}}(\rho)$ is given by (15).

Denote now as $P_{\text{CD}}^{(i)}(\delta, Q_i)$ the final CD probability at the CH of the ith cluster, conditioned on the target position δ and on the number of nodes Q_i in the ith cluster: in other words, $P_{\text{CD}}^{(i)}(\delta, Q_i)$ is the CD probability achieved by fusing all the received reports at the ith CH. Taking into account the fusion rules outlined in Section 2.4, one can write:

$$P_{\text{CD}}^{(i)}(\delta, Q_i) = \sum_{k=T_{\text{CH}}}^{Q_i}\binom{Q_i}{k}\left[\overline{P}_{\text{CD}}(r_i(\delta))\right]^k\left[1 - \overline{P}_{\text{CD}}(r_i(\delta))\right]^{Q_i-k} \tag{20}$$

where T_{CH} has been introduced in (11). By averaging over the number Q_i of elements in the ith cluster, one obtains:

$$P_{\text{CD}}^{(i)}(\delta) = \sum_{n=0}^{N} P_{\text{CD}}^{(i)}(\delta, n)p_n \tag{21}$$

where p_n is given by (5).

It is now possible to get the final CD probability $P_{\text{CD}}^{(f)}(\delta)$ at the C2 conditioned on δ. To this aim, denote: $\mathcal{N}_c = \{1,\ldots,N_c\}$, i.e., the set of integers indexing all the clusters in the network; $\mathcal{A}(m,k)$ as the set of integers containing the mth combination, out of all

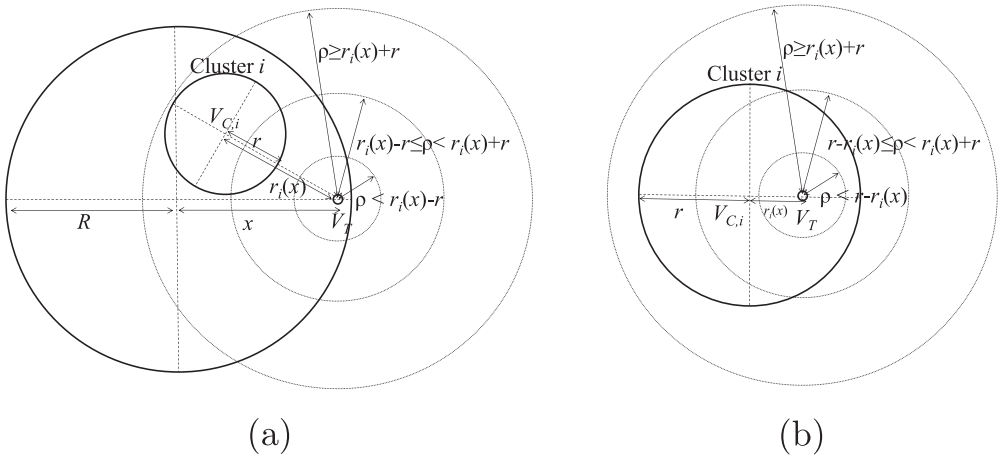

Fig. 2. Computation of $f_d(\rho|r_i(x))$: (a) the target is outside the cluster; (b) the target is inside the cluster.

possible combinations of elements in $\mathcal{N}_c$ taken k at a time, with $m = 1, \ldots, \binom{N_c}{k}$ and $k = 0, \ldots, N_c$; $\mathcal{A}'(m,k)$ as the complementary set of $\mathcal{A}(m,k)$, i.e., the set of all elements in $\mathcal{N}_c$ which are not in $\mathcal{A}(m,k)$. Using the introduced notations, one obtains:

$$P_{\mathrm{CD}}^{(f)}(\delta) = \sum_{k=T_{C2}}^{N_c} \sum_{m=1}^{\binom{N_c}{k}} \prod_{i \in \mathcal{A}(m,k)} P_{\mathrm{CD}}^{(i)}(\delta) \prod_{i \in \mathcal{A}'(m,k)} \left[1 - P_{\mathrm{CD}}^{(i)}(\delta)\right]. \tag{22}$$

Taking into account the PDF in (16), from (22) the unconditional CD probability at the C2 can be expressed as follows:

$$P_{\mathrm{CD}}^{(f)} = 2 \int_0^1 P_{\mathrm{CD}}^{(f)}(\delta) \delta \, \mathrm{d}\delta. \tag{23}$$

We now turn our attention to the FA probability. Since, in this case, the local decisions (at the sensors) do not depend on the position of the target, it can be concluded that the FA probability is the same for all clusters. Hence, denoting by $P_{\mathrm{FA}}(Q_i)$ the FA probability at the ith CH conditioned on the number of sensors Q_i in the cluster, one has:

$$P_{\mathrm{FA}}(Q_i) = \sum_{k=T_{\mathrm{CH}}}^{Q_i} \binom{Q_i}{k} (P_{\mathrm{FA}})^k (1 - P_{\mathrm{FA}})^{Q_i - k}. \tag{24}$$

By averaging over the number Q_i of elements in the ith cluster, taking into account the distribution of the number of nodes per cluster given by (5), the average FA probability at each CH can be expressed as follows:

$$P_{\mathrm{FA}}^{(c)} = \sum_{n=0}^{N} P_{\mathrm{FA}}(n) p_n. \tag{25}$$

The final FA probability $P_{\mathrm{FA}}^{(f)}$ at the C2 thus becomes

$$P_{\mathrm{FA}}^{(f)} = \sum_{i=T_{C2}}^{N_c} \binom{N_c}{i} (P_{\mathrm{FA}}^{(c)})^i (1 - P_{\mathrm{FA}}^{(c)})^{N_c - i}. \tag{26}$$

It can be observed that, setting $N_c = 1$, the just derived analytical framework (in terms of CD and FA probabilities) for a scenario with clustering can be easily extended to evaluate the CD and FA probabilities in the absence of clustering. Indeed, in this case the PMF $\{p_n\}$ of the number of nodes in the single (network-wide) cluster in (5) reduces to

$$p_n = \begin{cases} 1 & \text{if } n = N \\ 0 & \text{otherwise} \end{cases}$$

which corresponds to the case with a fixed number (N) of nodes in the cluster. Moreover, in this case the single cluster $V_{C,1}$ is located at the origin of the ROI and, accordingly, $r_i(\delta) = \delta$. We remark that, given the model considered in Section 2, the CD and FA probabilities obtained in the unclustered scenario are exact (there is no analytical approximation).

3.2.3. Energy consumption

Leveraging the previous analysis, the goal of this section is to derive the per-node average energy consumption as a function of the detection performance. In fact, sensors consume energy when they perform target detection and, therefore, they have data to be transmitted to the final collector. In particular, we distinguish between the cases with the presence ($S = S_1$) and absence ($S = S_0$) of the target.

Let us first consider *the case with* $S = S_1$, i.e., when the target is present in the ROI, and assume to have a clustered network, i.e., $N_c > 1$. Denote by $\overline{E}_S^{(1)}(i,\delta)$ the average energy consumption of a sensor node in ith cluster, conditioned on the position δ of the target. Hence, referring to the results derived in Section 2.3 and Section 3.2.2, one can write

$$\overline{E}_S^{(1)}(i,\delta) = E_{S,1} \overline{P}_{\mathrm{CD}}(r_i(\delta)) + E_{S,0}\left[1 - \overline{P}_{\mathrm{CD}}(r_i(\delta))\right]. \tag{27}$$

Denote by $\overline{E}_{\mathrm{CH}}^{(1)}(i,\delta,n)$ the average energy consumption of the CH in the ith cluster, conditioned on the target position δ and on the number of nodes n in the cluster. Leveraging again the results derived in Section 2.3 and Section 3.2.2, it follows:

$$\overline{E}_{\mathrm{CH}}^{(1)}(i,\delta,n) = E_{CH,1} P_{\mathrm{CD}}^{(i)}(\delta,n) + E_{\mathrm{CH},0}\left[1 - P_{\mathrm{CD}}^{(i)}(\delta,n)\right]. \tag{28}$$

Assume that, in each cluster, each node periodically becomes the CH (i.e., a rotation CH election strategy is used): this corresponds to assuming that each node has probability $1/n$ of becoming a CH, n being the number of nodes in the cluster. At this point, the average consumed energy per node in the ith cluster, conditioned on δ, can be expressed as:

$$\overline{E}_{\mathrm{avg}}^{(1)}(i,\delta) = \sum_{n=1}^{N} \left[\frac{n-1}{n} \overline{E}_S^{(1)}(i,\delta) + \frac{1}{n} \overline{E}_{\mathrm{CH}}^{(1)}(i,\delta,n)\right] p_n. \tag{29}$$

The overall network-wide per-node average energy consumption $\overline{E}_{\mathrm{avg}}^{(1)}$ can now be evaluated by averaging over (i) the clusters and (ii) the position δ of the target, thus obtaining:

$$\overline{E}_{\mathrm{avg}}^{(1)} = 2 \frac{1}{N_c} \int_0^1 \left[\sum_{i=1}^{N_c} \overline{E}_{\mathrm{avg}}^{(1)}(i,\delta)\right] \delta \, \mathrm{d}\delta. \tag{30}$$

Note that, in the absence of clustering, there is no CH and, hence, it is straightforward to derive the average per-node con-

sumed energy $\overline{E}_{\text{avg}}^{(1,f)}$ as follows:

$$\overline{E}_{\text{avg}}^{(1,f)} = 2\int_0^1 \left[E_{S,1}^{(f)}\overline{P}_{\text{CD}}(\delta) + E_{S,0}^{(f)}(1-\overline{P}_{\text{CD}}(\delta))\right]\delta\,\mathrm{d}\delta \tag{31}$$

where $\overline{P}_{\text{CD}}(\delta)$ can be evaluated by setting $N_{\text{c}} = 1$, as discussed at the end of Section 3.2.2.

The *case with* $S = S_0$ can be straightforwardly investigated by replacing P_{CD} with P_{FA}. In particular, in the clustered scenario one obtains:

$$\begin{aligned}\overline{E}_S^{(0)} &= E_{S,1}P_{\text{FA}} + E_{S,0}(1-P_{\text{FA}})\\ \overline{E}_{\text{CH}}^{(0)}(n) &= E_{CH,1}P_{\text{FA}}(n) + E_{\text{CH},0}[1-P_{\text{FA}}(n)]\\ \overline{E}_{\text{avg}}^{(0)} &= \sum_{n=1}^{N}\left[\frac{n-1}{n}\overline{E}_S^{(0)} + \frac{1}{n}\overline{E}_{\text{CH}}^{(0)}(n)\right]p_n.\end{aligned}$$

In the absence of clustering, the average per-node consumed energy can be expressed as follows:

$$\overline{E}_{\text{avg}}^{(0,f)} = E_{S,1}^{(f)}P_{\text{FA}} + E_{S,0}^{(f)}(1-P_{\text{FA}}). \tag{32}$$

4. Simulation-based performance evaluation

4.1. Parametric optimization

The analytical framework derived in Section 3 allows to evaluate the performance of the system in terms of CD/FA probabilities (and, then, energy consumption) as a function of a set of parameters that are not explicitly indicated in the CD/FA derivations to avoid abuse of notations. We quickly recall the following parameters embedded in the analytical framework:

- the transmit power P_{T} of the target;
- the noise power P_{N};
- the shadowing parameter σ and the path loss exponent α;
- the number m of samples in the acquisition phase at each sensor node;
- the ROI radius R (set to 1 in the analytical framework in Section 3);
- the number of nodes N and the number of clusters N_{c};
- the local decision threshold τ_N (at each sensor node) and the fusion thresholds T_{CH} (at CHs) and T_{C2} (at the C2).

While some of these parameters are out of control (namely, P_{T}, P_{N}, σ and α), the other parameters can be considered as design parameters and we adopt the following optimization strategy: upon fixing the parameters m, R, N, and N_{c}, the values of the thresholds τ_N, T_{CH} and T_{C2} are selected in order to optimize the performance.

In order to highlight the dependency of $P_{\text{CD}}^{(f)}$ and $P_{\text{FA}}^{(f)}$ on τ_N, T_{CH}, and T_{C2}, we introduce the following functions:

$$\begin{aligned}P_{\text{FA}}^{(f)} &= \mathcal{F}(\tau_N, T_{\text{CH}}, T_{\text{C2}})\\ P_{\text{CD}}^{(f)} &= \mathcal{G}(\tau_N, T_{\text{CH}}, T_{\text{C2}}).\end{aligned} \tag{33}$$

The threshold τ_N is then numerically evaluated through the following Neyman–Pearson approach. Denoting by $P_{\text{CD}}^{(\text{tgt})}$ the desired (network-wide) P_{CD}, for each possible value of τ_N we determine all possible threshold pairs $(T_{\text{CH}}^*, T_{\text{C2}}^*)$ which allow to achieve $P_{\text{CD}}^{(\text{tgt})}$, i.e.:

$$[T_{\text{CH}}^*(\tau_N), T_{\text{C2}}^*(\tau_N)] : \mathcal{G}(\tau_N, T_{\text{CH}}^*, T_{\text{C2}}^*) = P_{\text{CD}}^{(\text{tgt})}. \tag{34}$$

Hence, the optimal τ_N, denoted as τ_N^*, is selected as the value which allows to minimize $P_{\text{FA}}^{(f)}$, i.e.:

$$\tau_N^* = \arg\min_{\tau_N} F(\tau_N, T_{\text{CH}}^*(\tau_N), T_{\text{C2}}^*(\tau_N)). \tag{35}$$

To summarize, given a configuration of the input parameters (namely, P_{T}, P_{T}, σ, α, m, R, N, and N_{c}) and a value of the target CD probability $P_{\text{CD}}^{(\text{tgt})}$, the decision/fusion thresholds are set to $\left[\tau_N^*, T_{\text{CH}}^*(\tau_N^*), T_{\text{C2}}^*(\tau_N^*)\right]$: this allows to minimize $P_{\text{FA}}^{(f)}$ and we will refer to this minimum as P_{FA}^*.

The following setup is considered for the performance analysis carried out in the next Section 4.2. The path-loss exponent α is set to 4 (assuming a strong attenuation, realistic for large-scale monitoring scenarios) and the shadowing parameter σ is set to 5 dB (a typical value for terrestrial propagation). As anticipated in Section 3, the radius R of the ROI is normalized to 1. Hence, we introduce the ratio $\gamma_0 = KP_{\text{T}}/P_{\text{N}}$ which, according to (2) and from the assumption of unitary radius $R = 1$, represents the average (averaged over the shadowing) SNR at a sensor located at distance 1 from the target. As for the IEEE 802.15.4 superframe structure, we consider that the number of time slots M is set to allow, on average, transmission from all sensors in the cluster during an active period, i.e., $M = \lceil N/N_{\text{c}} \rceil$. Then, we assume that the maximum number of measurements at each sensor node during a time slot is 16: in general, $m \leq 16$ observed consecutive measurements will be considered $(\{|\mu_k(\ell)|^2\}_{\ell=1}^m$, according to (3)), so that the relative sensing time during an active period can be written as $\beta = m/16$. Finally, the transmit power for long-range communications (between CH and C2) is assumed 20 times higher than P_M, i.e., $\gamma = 20$—typically, IEEE 802.15.4 node have a transmit power of 1 mW, whereas SubGHz node can transmit up to 300 mW (e.g., Xbee PRO 868 RF modules, http://ftp1.digi.com/support/documentation/90001020_F.pdf).

4.2. Comparative performance evaluation

We now present performance results with the aim of providing a comprehensive comparison between clustered and unclustered network topologies. As the analytical framework developed in Section 3 provides an approximate (average) performance evaluation, we also show Monte Carlo simulation-based performance results. In this case, the CD/FA probabilities and the energy consumption are obtained by averaging over different network topology realizations. In particular, at each simulation run, the positions of sensors and of the target are randomly selected in the ROI (this guarantees various realizations for the received powers at the sensors); then, clusters are formed using the well-known k-means algorithm [14,15] and the CH is randomly chosen among the nodes of a cluster.[2] Simulations have been performed so that the 95% of confidence interval is achieved. The confidence interval is denoted in the following by a vertical bar around the simulation point.

We first investigate the per-node average consumed energy normalized to $P_{\text{M}}T_M$, i.e., normalized to the energy for transmitting/receiving/sensing over a single slot. More precisely, the normalized energy is evaluated as a function of: the target network-wide Missed Detection (MD) probability $P_{\text{MD}}^{(\text{tgt})} = 1 - P_{\text{CD}}^{(\text{tgt})}$ (in Fig. 3) and the minimum network-wide FA probability $P_{\text{FA}}^{(*)}$ (in Fig. 4). In both figures, clustered scenarios with $N_{\text{c}} = 4$ clusters are assumed. The performance results obtained through the analytical approach (solid lines) are directly compared with those obtained through simulations (dashed lines). In Fig. 3, four values for the number N of sensors in the ROI are considered (namely, 12, 24, 36, 48), whereas in Fig. 4, to avoid overlap among similar curves, only the two limiting values of N are considered (namely, 12 and 48). In both figures, m is set to 8, i.e., $\beta = 0.5$. It can be observed that the analytical curves quite tightly upper bound the simulation-

[2] We remark that cluster formation goes beyond the scope of this paper. The use of the k-means algorithm is reasonable, assuming an initial set-up phase when the sensor nodes are deployed on the field.

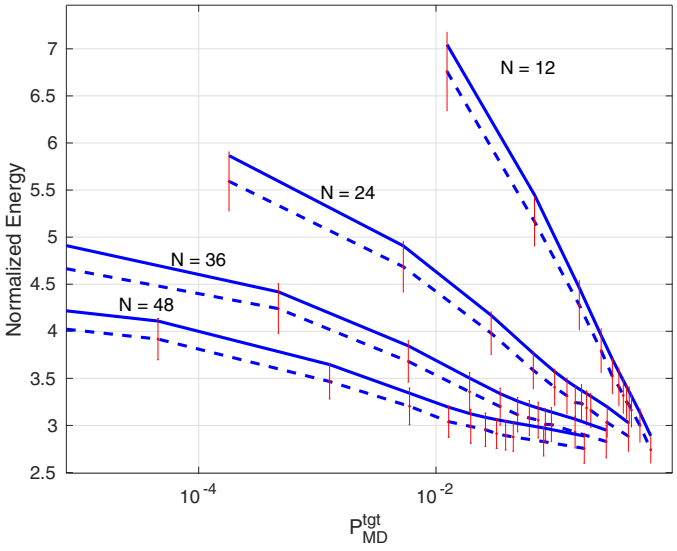

Fig. 3. Average per-node consumed energy as a function of the target MD probability. Various values of the number of nodes N are considered. For each value of N, analytical (solid lines) and simulation (dashed lines) results are presented. In all cases, $N_c = 4$ and $m = 8$ ($\beta = 0.5$).

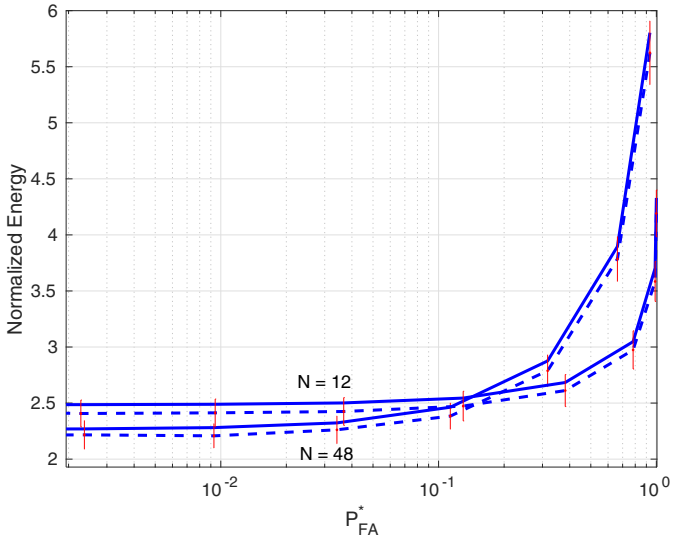

Fig. 4. Average per-node consumed energy as a function of the minimum reachable FA probability. Two values of the number of nodes N are considered. For each value of N, analytical (solid lines) and simulation (dashed lines) results are presented. In all cases, $N_c = 4$ and $m = 8$ ($\beta = 0.5$).

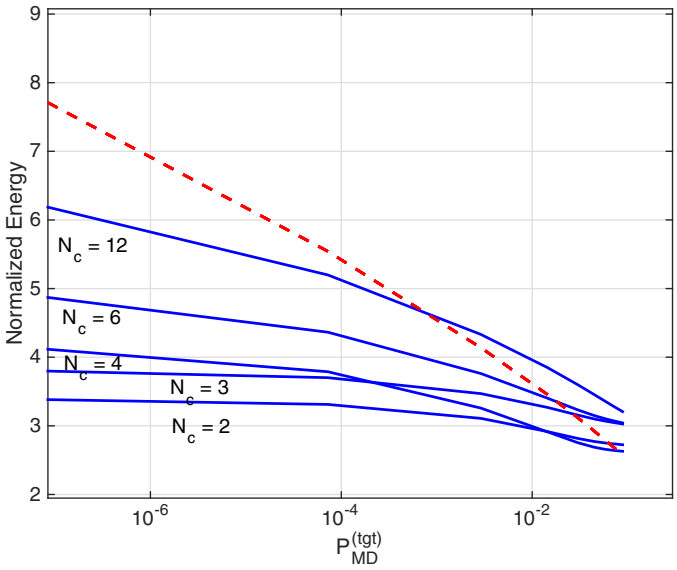

Fig. 5. Average per-node consumed energy as a function of the target MD probability, for both clustered (solid lines) and unclustered (dashed line) scenarios. In the clustered case, various values of the number of clusters N_c are considered. In all cases, $N = 48$ and $m = 8$ ($\beta = 0.5$).

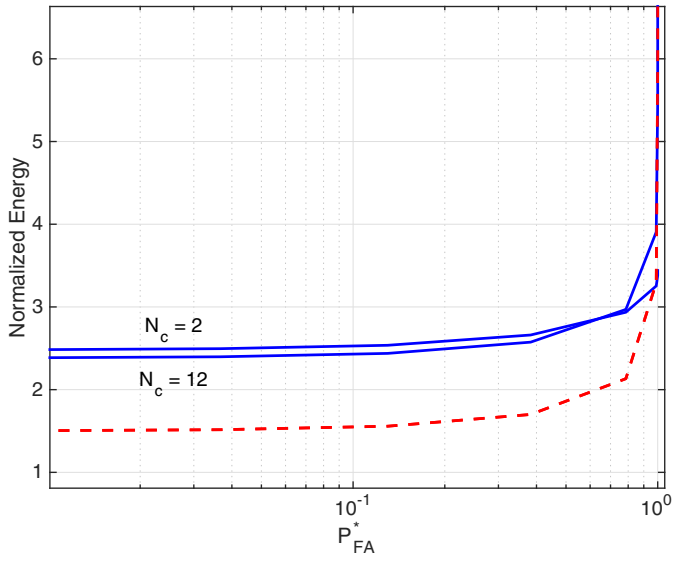

Fig. 6. Average per-node consumed energy as a function of the minimum achievable FA probability, for both clustered (solid lines) and unclustered (dashed line) scenarios. In the clustered case, various values of the number of clusters N_c are considered. In all cases, $N = 48$ and $m = 8$ ($\beta = 0.5$).

based results, thus validating the analytical framework proposed in Section 3. The same accuracy is achieved also for different parameter settings, which are omitted here for the sake of conciseness. From the results in Fig. 3 it can be observed, as intuitively expected, that the energy consumption is a decreasing function of the MD probability: in other words, in order to achieve a better performance in terms of CD probability (namely, to lower the MD probability) it is necessary to spend more energy. On the other hand, for a given CD probability, increasing the number N of sensors allows to decrease the required energy. Indeed, increasing the number of sensors in the ROI allows to guarantee a better coverage of the area if interest and, ultimately, allows to improve the system performance in terms of target detection capabilities. Considering the FA probability (Fig. 4), the results need some further discussion. Indeed, in this case the consumed energy tends to decrease for decreasing values of the FA probability and of the number of sensors: in other words, the performance improves for lower energy consumption and fewer sensors. This is not surprising: in fact, increasing the number of sensors increases the probability of correctly detecting a target at the cost of higher consumed energy.

Having validated the accuracy of the proposed analytical framework for performance evaluation, this framework can be exploited to investigate further the impact of clustering on the system performance. More precisely, fixing the number N of sensors in the ROI to 48 and the relative sensing interval β to 0.5, we investigate the impact of the number of clusters N_c. In Fig. 5, the average per-node consumed energy is shown as a function of the target MD probability for various values of N_c (namely, 2, 3, 4, 6, 12), while in Fig. 6 the consumed energy is shown as a function of the minimum FA probability, considering only the limiting values

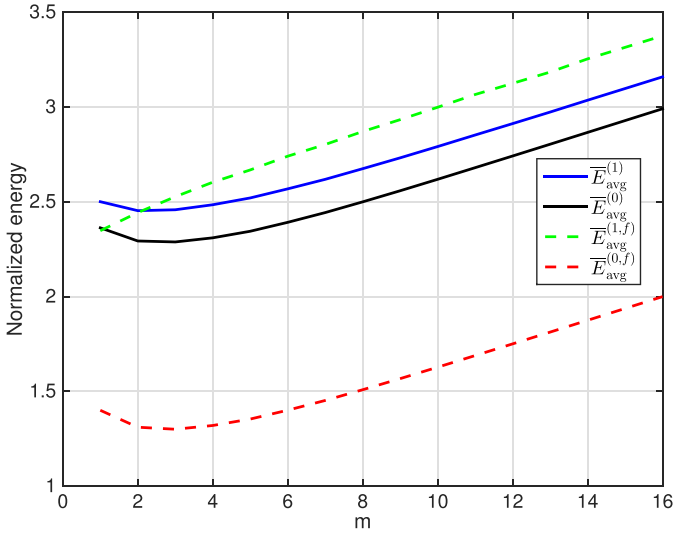

Fig. 7. Average per-node consumed energy, for both S_1 and S_0 cases, as a function of the number of sensed samples m: comparison between clustered ($N_c = 4$, solid lines) and unclustered (dashed lines) scenarios. In all cases, $P_{\text{MD}}^{(\text{tgt})} = 0.02$ and $N = 48$.

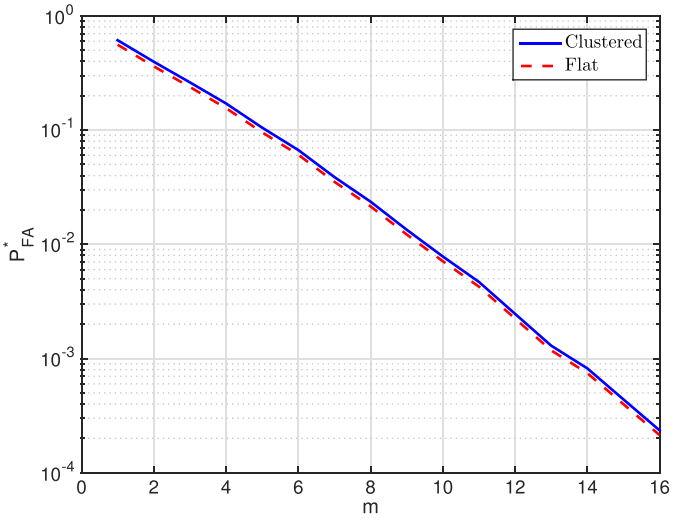

Fig. 8. Minimum achievable FA probability as a function of the number of sensed samples m: comparison between clustered ($N_c = 4$, solid line) and unclustered (dashed line) scenarios. In all cases, $P_{\text{MD}}^{(\text{tgt})} = 0.02$ and $N = 48$.

of N_c in the previous figure (namely, 2 and 12). For comparison purposes, in the two figures we also report the results obtained in the unclustered scenario (dashed curve). With reference to the MD probability (see Fig. 5), it is worth noting that the choice of the best clustering setting, i.e., the best value of N_c, depends on the required CD probability. Indeed, for stringent requirements, i.e., very low $P_{\text{MD}}^{(\text{tgt})}$, it is preferable to have a smaller number of clusters, whereas for looser requirements it may be convenient to increase N_c. The rationale for this behavior lies in the trade-off, at the CH, between the following tendencies: (*i*) the smaller N_c, the larger the number of sensors in the cluster, i.e., the higher M and, accordingly, the higher the energy consumption for managing the cluster; (*ii*) the larger N_c, the larger the number of transmissions towards the C2, i.e., the higher the consumed energy. Hence, when the CD probability is high, the number of transmissions towards C2 is large and the behavior described in (*ii*) is the major source of energy consumption. On the other hand, the opposite situation occurs for lower values of the CD probability. As for the unclustered scenario, it is worth noting that for low MD (equivalently, high CD) probabilities the performance is worse than in the clustered cases, while the opposite situation occurs for looser CD probability requirements. This behavior is due to the fact that the higher the target detection probability, the higher the effect of long-range communications in determining the total consumed energy. Concerning the FA probability (see Fig. 6), it can be observed that for reasonably low value of the FA probability, the unclustered case allows to achieve a lower consumed energy with respect to the clustered cases. This is due to the fact that in this case the number of transmissions towards the C2 is not the major source of energy consumption. The situation is somehow different for high FA probability (i.e., $P_{\text{FA}}^{(*)}$ close to 1), which, however, is not a case of practical interest. Eventually, increasing the number of clusters allows to save energy for low $P_{\text{FA}}^{(*)}$, which is a situation where the case (*i*) described above has a higher effect in determining the total consumed energy. On the contrary, for high values of $P_{\text{FA}}^{(*)}$ the energy decreases by decreasing N_c, since, in this case, the number of transmissions towards the C2 increases.

In the next two figures we show the effect of the number of sensed samples m on both the energy consumption (Fig. 7) and the minimum achievable FA probability $P_{\text{FA}}^{(*)}$ (Fig. 8), for a predefined target MD probability $P_{\text{MD}}^{(\text{tgt})} = 0.02$. In both figures, clustered ($N_c = 4$, solid lines) and unclustered scenarios are compared. In Fig. 7, the average consumed energies are evaluated in the cases $S = S_1$ (target presence) and $S = S_0$ (target absence) and, for each case, in both clustered and unclustered scenarios. In the S_1 case, the energies in the clustered ($\overline{E}^{(1)}_{\text{avg}}$) and unclustered ($\overline{E}^{(1,f)}_{\text{avg}}$) scenarios are increasing functions of m: this is an expected result since, in this case, setting the CD probability corresponds, approximately, to setting the report transmission rate and, hence, the term which mainly influences the final consumed energy is the sensing period interval. In the S_0 case, instead, increasing m has a two-fold effect: on one hand, it increases the time spent to sense the channel; on the other hand, it allows to noticeably decrease the FA probability (as shown in Fig. 8) and this, ultimately, tends to decrease the consumed energy. As a matter of fact, we observe that for low values of m the energy is a decreasing function of m, whereas increasing m the effect of increasing the sensing period overcomes the second effect (FA probability reduction). From the comparison between the clustered and unclustered scenarios, it turns out that clustering allows to save energy in the case S_1, while the opposite occurs in the case S_0. From the results in Fig. 8, it can be concluded that the clustered and unclustered scenarios behave almost identically in terms of P^*_{FA}.

5. Concluding remarks

In this paper, we have considered WSN-based surveillance scenarios, where sensor nodes cooperate to detect the presence of an unwanted target node over a ROI. Leveraging recent results in cognitive wireless networking, we have first introduced the system model, encompassing unclustered and clustered cases. Proper decision rules (at the single sensors) and fusion rules (at CHs and C2) have been derived. An innovative analytical performance evaluation framework has then been proposed, leading to an efficient parametric optimization (in terms of decision and fusion thresholds). The accuracy of the proposed analytical framework has been confirmed through simulation-based results. The obtained results, by quantifying inherent trade-offs between the per-node consumed energy, topology (clustered/unclustered), FA/CD/MD probabilities, and sensing duration, provide useful design guidelines.

While in the current work the positions of the target and the sensor nodes are assumed to be unknown, future work will focus on the extension of the current framework exploiting side informa-

tion, namely, knowledge of the positions of sensor nodes (as this is a very reasonable assumption in surveillance systems). Moreover, the use of different fusion rules, exploiting this side information and/or multi-level quantization at the sensors, represents an interesting future research direction.

References

[1] I. Butun, S.D. Morgera, R. Sankar, A survey of intrusion detection systems in wireless sensor networks, IEEE Commun. Surv. Tutorials 16 (1) (2014) 266–282.

[2] P. Medagliani, J. Leguay, G. Ferrari, V. Gay, M. Lopez-Ramos, Energy-efficient mobile target detection in Wireless Sensor Networks with random node deployment and partial coverage, Elsevier Pervasive Mobile Comput. 8 (3) (2012) 429–447.

[3] T. Clouqueur, K.K. Saluja, P. Ramanathan, Fault tolerance in collaborative sensor networks for target detection, IEEE Trans. Comput. 53 (3) (2004) 320–333.

[4] C.C. Hsu, Y.Y. Chen, C.F. Chou, L. Golubchik, On design of collaborative mobile sensor networks for deadline-sensitive mobile target detection, IEEE Sens. J. 13 (8) (2013) 2962–2972.

[5] T.L. Chin, W.C. Chuang, Latency of collaborative target detection for surveillance sensor networks, IEEE Trans. Parallel Distrib. Syst. 26 (2) (2015) 467–477.

[6] Y. Zou, K. Chakrabarty, Target localization based on energy considerations in distributed sensor networks, in: Proc. IEEE Int. Workshop on Sensor Network Protocols and Applications (SNPA), 2003, pp. 51–58. Anchorage, AK, USA

[7] D. Ding, Z. Wang, D.W.C. Ho, G. Wei, Observer-based event-triggering consensus control for multiagent systems with lossy sensors and cyber-attacks, IEEE Trans. Cybern. (2016). to appear.

[8] D. Ding, Z. Wang, B. Shen, H. Dong, Event-triggered distributed $\mathcal{H}_\infty$ state estimation with packet dropouts through sensor networks, IET Control Theory Appl. 9 (13) (2015) 1948–1955.

[9] D. Ding, Z. Wang, B. Shen, G. Wei, Event-triggered consensus control for discrete-time stochastic multi-agent systems, Automatica 62 (2015) 284–291.

[10] R. Tandra, M. Mishra, A. Sahai, What is a spectrum hole and what does it take to recognize one? Proc. IEEE 97 (2009) 824–848.

[11] A. Abrardo, M. Martalò, G. Ferrari, Impact of the knowledge of nodes' positions on spectrum sensing strategies in cognitive networks, Elsevier Phys. Commun. 19 (2016) 84–92.

[12] M. Kaczurova, J. Vesely, M. Kaczur, Analysis of possibilities to target detection by using secondarily emitted signals, in: Int. Conf. Military Technologies (ICMT), 2015, pp. 1–4. Brno, Czech Republic

[13] S. Aust, T. Ito, Sub 1ghz wireless LAN propagation path loss models for urban smart grid applications, in: IEEE Int. Conf.Computing, Networking and Communications (ICNC), 2012, pp. 116–120. Maui, HI, USA

[14] S. Lloyd, Least squares quantization in pcm, IEEE Trans. Inform. Theory 28 (2) (1982) 129–137.

[15] D. Arthur, S. Vassilvitskii, K-means++: The advantages of careful seeding, in: Proc. ACM-SIAM Symposium on Discrete Algorithms (SODA), 2007, pp. 1027–1035. New Orleans, LA, Louisiana

[16] Q. Zhao, A. Swami, Cognitive Radio Communications and Networks, Academic Press.Ed.: A.M. Wyglinski, M. Nekovee, Y.T. Hou.

[17] A. Goldsmith, Wireless Communications, Cambridge University Press, 2005. New York, NY, USA.

[18] S.M. Kay, Fundamentals of Statistical Signal Processing: Estimation Theory, Prentice-Hall, 1993. Upper Saddle River, NJ.

[19] E. Karapistoli, F. Pavlidou, I. Gragopoulos, I. Tsetsinas, An overview of the IEEE 802.15.4a standard, IEEE Commun. Mag. (2010) 47–53.

[20] S. Pollin, M. Ergen, S.C. Ergen, B. Bougard, Performance analysis of slotted carrier sense ieee 802.15.4 medium access layer, IEEE Trans. Wireless Commun. 7 (9) (2008) 3359–3371.

[21] A. Abrardo, L. Balucanti, A. Mecocci, A game theory distributed approach for energy optimization in WSNs, ACM Trans. Sen. Netw. 9 (4) (2013) 1–22.

[22] J. Polastre, R. Szewczyk, D. Culler, Telos: enabling ultra-low power wireless research, in: Int. Symposium Info. Proc. Sensor Networks (IPSN), 2005, pp. 364–369. Los Angeles, CA, USA

[23] A. Abrardo, M. Martalò, G. Ferrari, Multisensor Data Fusion: From Algorithm and Architecture Design to Applications, CRC Press.Ed.: H. Fourati, K. Iniewski.

[24] M. Abramowitz, I.A. Stegun (Eds.), Handbook of Mathematical Functions, Dover, 1982.